High-Volume-Rate 3-D Ultrasound Imaging Using Fast-Tilting and Redirecting Reflectors

Zhijie Dong, *Graduate Student Member, IEEE*, Shuangliang Li, Xiaoyu Duan, Matthew R. Lowerison, Chengwu Huang, Qi You, *Graduate Student Member, IEEE*, Shigao Chen, *Senior Member, IEEE*, Jun Zou, *Senior Member, IEEE*, and Pengfei Song, *Senior Member, IEEE*

***Abstract*—Three-dimensional ultrasound imaging has many advantages over 2-D imaging such as more comprehensive tissue evaluation and less operator dependence. However, developing a low-cost and accessible 3-D ultrasound solution with high volume rate and imaging quality remains a challenging task. Recently, we proposed a 3-D ultrasound imaging technique: fast acoustic steering via tilting electromechanical reflectors (FASTER), which uses a fast-tilting acoustic reflector to steer ultrafast plane waves elevationally to achieve high-volume-rate 3-D imaging with conventional 1-D transducers. However, the initial FASTER implementation requires a water tank for acoustic wave conduction and cannot be conveniently used for regular handheld scanning. To address these limitations, here, we developed a novel ultrasound probe clip-on device that encloses a fast-tilting reflector, a redirecting reflector, and an acoustic wave conduction medium. The new FASTER 3-D imaging device can be easily attached to or removed from clinical ultrasound transducers, allowing rapid transformation from 2-D to 3-D imaging. In vitro B-mode studies demonstrated that the proposed method provided comparable imaging quality to conventional, mechanical-translation-based 3-D imaging while offering a much faster volume rate (e.g., 300 versus ~10 Hz). We also demonstrated 3-D power Doppler (PD) and 3-D super-resolution ultrasound localization microscopy (ULM) with the FASTER device. An in vivo imaging study showed that the FASTER device could clearly visualize the 3-D anatomy of the basilic vein. These results suggest that the newly developed redirecting reflector and the clip-on device could overcome key hurdles for future clinical translation of the FASTER 3-D imaging technology.**

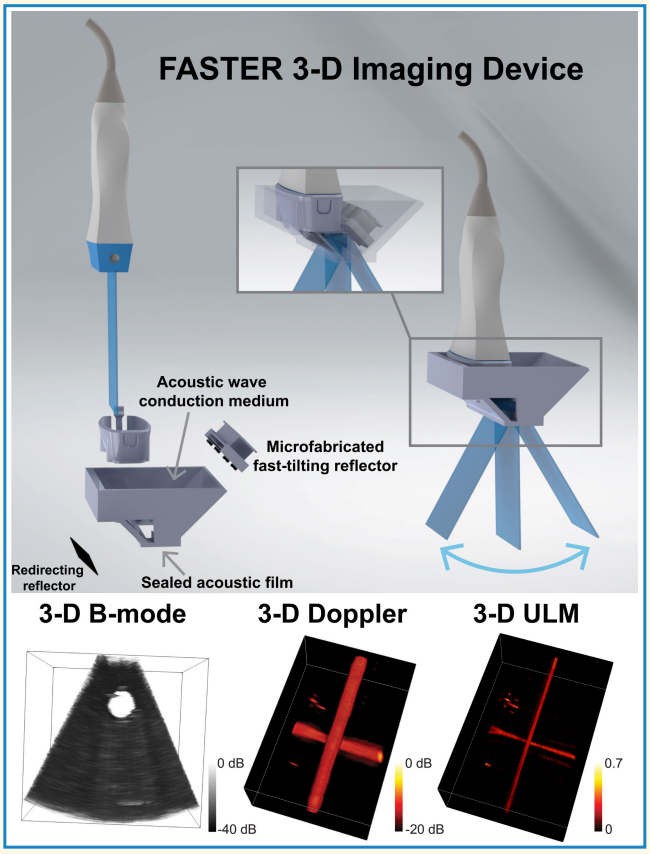

***Index Terms*—3-D ultrafast imaging, 3-D ultrasound imaging, 3-D ultrasound localization microscopy (ULM), acoustic reflector, microfabrication.**

I. Introduction

ULTRASOUND is a widely available and accessible medical imaging modality due to its safety, real-time imaging speed, portability, and low cost. One of the significant advantages of ultrasound imaging is its ultrafast imaging capability due to short pulse-echo time (e.g., ~0.1 ms), and the exploration of ultrafast ultrasound (e.g., 1000-Hz frame rate) can be traced back to the 1970 s and 1980 s by using analog parallel processing [1], [2] and defocused beam [2]. In the last two decades, driven by the rapid growth of compounding plane wave imaging-based ultrafast imaging technologies [3], [4], [5], many advanced ultrasound imaging techniques, such as shear wave elastography (SWE) [6], functional ultrasound (fUS) [7], and super-resolution ultrasound localization microscopy (ULM) [8], have been rapidly emerging. These imaging techniques provided new biomarkers that created numerous unprecedented possibilities in many preclinical and clinical applications [9].

Manuscript received 20 March 2023; accepted 30 May 2023. Date of publication 5 June 2023; date of current version 2 August 2023. This work was supported by the National Institute of Biomedical Imaging and Bioengineering of the National Institutes of Health under Award R01EB031040. *(Corresponding author: Pengfei Song.)*

This work involved human subjects or animals in its research. The authors confirm that all human/animal subject research procedures and protocols are exempt from review board approval.

Please see the Acknowledgment section of this article for the author affiliations.

Digital Object Identifier 10.1109/TUFFC.2023.3282949

Highlights

- **A new version of the FASTER probe clip-on device was developed, which enables high volume-rate, multimodal 3-D ultrasound imaging with regular 1-D ultrasound probes.**
- **The FASTER device provides multimodal imaging capability with comparable imaging quality to conventional mechanical-scanning-based 3-D imaging while offering a significantly higher volume rate.**
- **FASTER presents a low-cost, user-friendly, accessible, and functional solution for 3-D ultrasound imaging.**

Despite the rapid development of ultrasound imaging, the majority of ultrasound scans being performed are still 2-D. This forms one of the key challenges of ultrasound imaging because the 2-D scanning is operator-dependent and may not provide a comprehensive evaluation of the targeted tissue. Furthermore, one of the major functions of ultrasound imaging is to detect motions (e.g., blood flow, shear wave, and microbubble flow), which propagate in all three dimensions and cannot be fully captured with 2-D scans. This results in inaccurate quantifications of biomarkers such as blood flow velocity and shear wave speed if the blood flow and shear wave motion have out-of-plane components [10], [11]. Moreover, 3-D ultrasound scanning is also beneficial for many intraoperative and interventional procedures that use ultrasound images for guidance [12], [13], [14], [15].

Although 3-D ultrasound imaging systems are present in the clinic for echocardiography [16], [17], [18], surgical guidance [19], obstetrics [17], and vascular imaging [20], their performance and functionality are limited by high equipment costs (e.g., 2-D matrix arrays), being cumbersome to use (e.g., wobblers), and low scanning volume rates. For example, the most popular clinical 3-D ultrasound solution is based on "wobblers" that mechanically sweep a 1-D probe to collect 2-D imaging slices that are stacked into 3-D volumes [21]. However, this inevitably results in bulky devices and is limited to very slow scanning speed (e.g., several volumes per second). Another 3-D imaging solution is based on 2-D matrix arrays, which support electronic scanning of large 3-D volumes at a much higher volume rate (e.g., tens of hertz). However, 2-D matrix arrays are expensive and only available on high-end ultrasound systems for specialty applications in the clinic. Furthermore, due to a large number of transducer elements and channels, 2-D matrix arrays are also associated with high computational costs (e.g., beamforming). As such, multiplexing [22] or micro-beamforming [23] are typically necessary for practical implementations of 2-D matrix arrays. Nevertheless, the 3-D volume rate is compromised due to the need for multiple pulse-echo cycles to reconstruct a full 3-D volume. Although emerging techniques, such as sparse arrays [24] and row-column addressing (RCA) arrays [25], [26], [27], [28], present promising solutions for high-volume-rate 3-D scanning, each of them has its own challenges and still requires further development.

Recently, we have investigated a new ultrasound scanning technique, called fast acoustic steering via tilting electromechanical reflectors (FASTER) [29], which uses a water-immersible and fast-tilting acoustic reflector [30] to achieve low-cost and high-volume-rate 3-D scanning by rapidly steering ultrafast plane waves in the elevational direction. Through acquiring 2-D slices at different elevational positions, 3-D volumes can be reconstructed using scan conversion (i.e., converting and interpolating batches of 2-D slices sampled in polar coordinates to volumes in Cartesian coordinates). FASTER 3-D imaging does not need 2-D matrix arrays and can be directly applied to conventional 1-D array transducers. This allows the system to fully benefit from linear probes' superior performance (e.g., bandwidth, signal-to-noise ratio (SNR), shielding, coupling, and matching) over matrix arrays, due to optimal linear array fabrication. Unlike the wobbler, FASTER sweeps the ultrasound beam instead of the ultrasound transducer, thereby enabling a much faster 3-D scanning speed (e.g., hundreds of hertz). Another advantage of FASTER over wobblers is that because FASTER does not sweep the transducer, it does not use a motor and thus can have a much more compact and lightweight form factor. However, one limitation was that since the fast-tilting reflector alters the ultrasound wave propagation direction (i.e., from axial to elevational propagation), the ultrasound probe could not be held in the regular position.

In this study, a second acoustic reflector (i.e., a redirecting reflector) was added to recover the axial acoustic wave propagation direction, which allows the transducer to be held in a regular upright position by the operator. In addition, a compact and lightweight clip-on housing device was designed and fabricated to enclose both reflectors and the acoustic wave coupling medium. As a result, the new FASTER clip-on device can be easily attached to or removed from conventional 1-D array transducers. Both in vitro and in vivo studies were conducted to evaluate the 3-D imaging capabilities of the new FASTER 3-D imaging device. The application of high-volume-rate 3-D scanning was also demonstrated with 3-D power Doppler (PD) and 3-D ULM experiments.

The rest of this article is structured as follows. We first describe the design of the new FASTER 3-D clip-on device and related image reconstruction processes. We then present validation and calibration, followed by in vitro and in vivo imaging studies. We finalize this article with discussions and conclusions.

II. Materials and Methods

A. Principles of FASTER 3-D Imaging

The proposed FASTER technique takes advantage of the ultrafast frame rate of plane wave imaging [3] (e.g., thousands of hertz to tens of thousands of hertz) and rapidly distributes ultrasound beams at different elevational locations using a water-immersible and microfabricated fast-tilting reflector [29]. In the previous design, the imaging direction was orthogonal to the conventional axial imaging direction

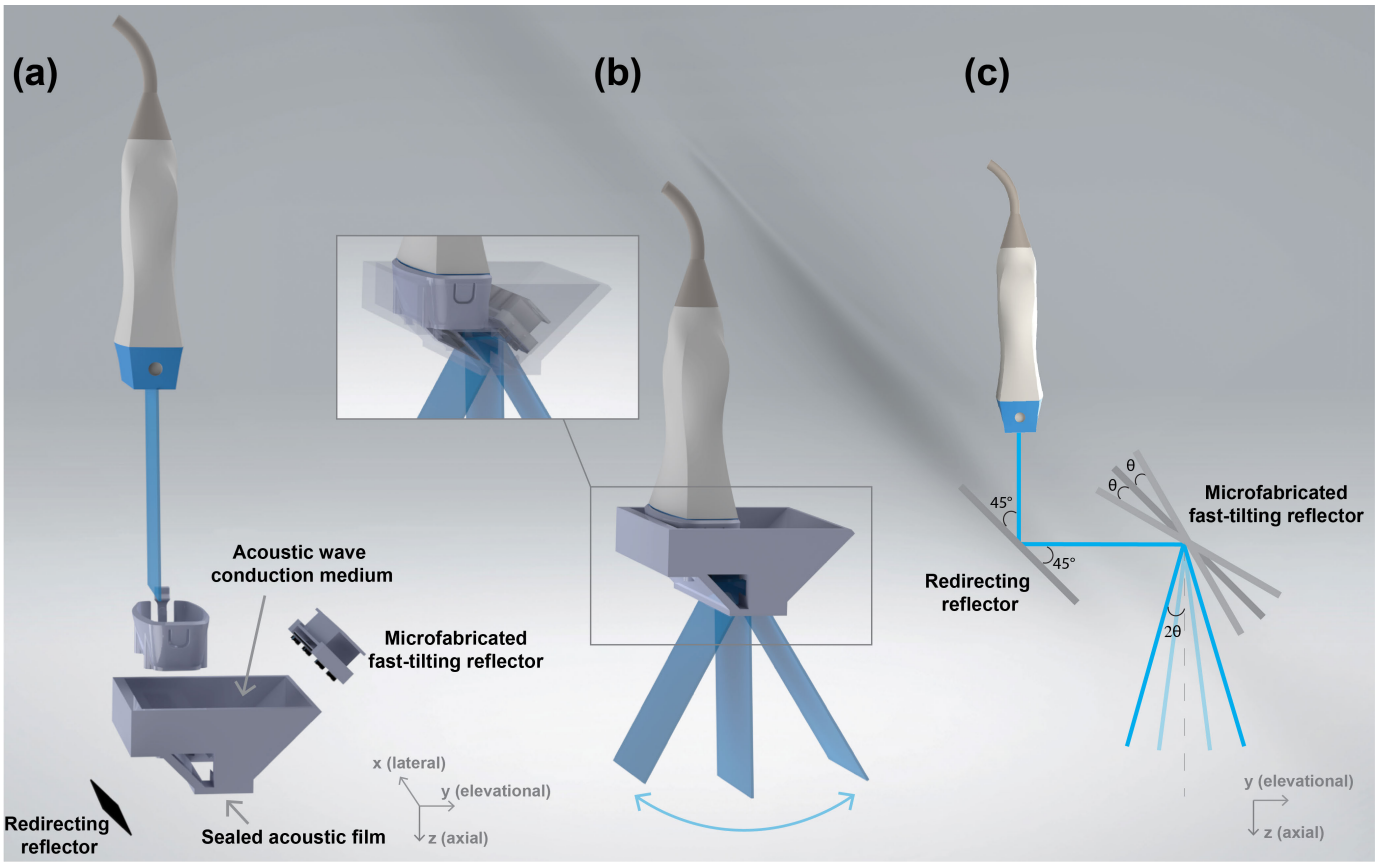

Fig. 1. FASTER 3-D imaging device schematics. (a) Components of the new FASTER 3-D imaging device: conventional 1-D ultrasound probe and clip-on housing device, which encloses a redirecting reflector, a fast-tilting reflector (driven by two electromagnet coils), acoustic wave conduction medium, and an acoustic film (on the bottom) for sealing. (b) FASTER 3-D scanning schematics. The FASTER device rapidly distributes ultrasound beams at different elevational locations using the fast-tilting reflector. (c) Acoustic reflection path of the FASTER 3-D imaging device. The ultrasound beam is reflected by the redirecting reflector first by 90°, followed by another reflection by the fast-tilting reflector.

because the fast-tilting reflector bends the ultrasound beam by 90°. To allow the transducer to be held in a regular position (e.g., upright), a redirecting reflector was added prior to the fast-tilting reflector to recover the axial incident beam direction (Fig. 1). The ultrasound beam is first reflected by the redirecting reflector by 90°(from axial propagation to elevational), followed by another 90° reflection by the fast-tilting reflector (from elevational back to axial). The redirecting and fast-tilting reflectors were made of the same silicon wafer, which provides high acoustic reflectivity due to the high acoustic impedance and smooth surface. The redirecting reflector was parallel to the stationary position of the fast-tilting reflector (i.e., tilted by 45° to the incident beam direction), as shown in Fig. 1(c).

To address the limitation of needing a water tank in the previous FASTER setup, a compact clip-on housing device was designed. The clip-on housing device encloses the reflectors and acoustic wave conduction medium (water at room temperature) with a sealing acoustic film [polyvinyl chloride (PVC)] attached to the bottom [see Fig. 1(a) and (b)]. Three-dimensional printing was used to fabricate the clip-on housing device frame using polylactic acid (PLA). The net weight of the device frame was 26 g, and the total weight, including both reflectors, was 57 g. An adapter was 3-D printed to allow a GE 9LD transducer (GE Healthcare, Wauwatosa, WI, USA) to be easily attached to or removed from the FASTER device [Fig. 1(a)]. The detailed design parameters are reported in Table I.

TABLE I
SPECIFICATION OF THE FASTER DEVICE DESIGNED FOR THE GE 9LD LINEAR ARRAY TRANSDUCER

Parameter	Value
Clip-on housing device weight (including reflectors) [g]	57
Clip-on housing device size ($l \times w \times h$) [mm^3]	$74.8 \times 59.8 \times 30.9$
Redirecting reflector size ($l \times w \times h$) [mm^3]	$66.5 \times 17.0 \times 0.2$
Fast-tilting reflector size ($l \times w \times h$) [mm^3]	$48.4 \times 7.0 \times 0.2$
Electromagnet size [mm^2]	10.0 diameter × 25.0
Acoustic window size [mm^2]	50.9 lateral × 12.0 elevational
Acoustic film thickness [mm]	0.01
Power [W]	0.48

Similar to the imaging procedures introduced in our previous work [29], the 1-D ultrasound transducer and the fast-tilting reflector were synchronized by triggering the sinusoidal driving signal of the fast-tilting reflector with the ultrasound imaging system. The corresponding tilting angles [e.g., θ in Fig. 1(c)] at each elevational location were calibrated. Because the incident angle is equal to the reflection angle of an acoustic beam, the final elevational scanning angle

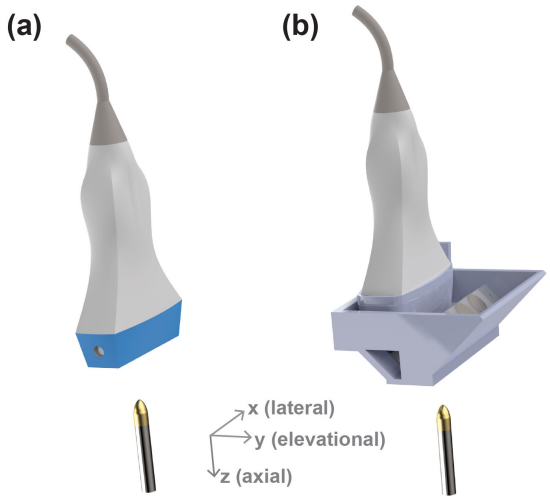

Fig. 2. Experimental setup of the acoustic validation study for the FASTER 3-D imaging device. A hydrophone was used to measure the 3-D acoustic field (a) without and (b) with the FASTER device. For the measurements with the FASTER device attached, the fast-tilting reflector was kept stationary during the experiment.

is 2θ after passing through two reflectors [Fig. 1(c)]. The raw ultrasound data sampled in polar coordinates were scan converted to Cartesian coordinates using 3-D natural neighbor interpolation [31].

B. Acoustic Validation Study of Ultrasound Beam Reflections

To evaluate the accuracy and efficacy of beam reflection by the redirecting reflector and the fast-tilting reflector, the acoustic field was carefully scanned and characterized using an acoustic intensity measurement system (AIMS III, Onda Corporation, Sunnyvale, CA, USA) with a capsule hydrophone (HGL-0200, Onda Corporation, Sunnyvale, CA, USA). Three-dimensional acoustic pressure fields were measured in two different setups, as shown in Fig. 2: 1) direct measurements from the ultrasound transducer without the FASTER device and 2) measurements with the FASTER device attached to the probe. For all the experiments, a Verasonics Vantage 256 system (Verasonics Inc., Kirkland, WA, USA) was used. The hydrophone was mounted on the linear and rotary positioners of the ONDA AIMS system to scan the 3-D acoustic field, with 0.2-, 1-, and 2-mm step size in the elevational, axial, and lateral dimensions, respectively. The Vantage system was synchronized with the capsule hydrophone and the scanning stage.

The hydrophone sampling frequency was 125 MHz, and the measured signals were processed using low-pass FIR filtering (a cutoff frequency of 10 MHz) and windowing. The acoustic beam characteristics (i.e., beamwidth and spectrum) were compared to examine whether any beam distortion occurred inside the FASTER device. The beamwidth was quantified using the full-width at half-maximum (FWHM).

C. Acoustic Calibration Study for Ultrasound Beam Scanning

To accurately reconstruct the volumetric images based on individual 2-D slices acquired at different scanning positions, the actual scanning angle of each 2-D imaging slice needs to be determined. Similar to the calibration process presented in the previous study [29], a second 1-D linear transducer (L7-4, ATL Philips, Bothell, WA, USA) was used to capture the dynamic 3-D scanning field of the FASTER 3-D imaging device, as shown in Fig. 3. The two 1-D transducers were synchronized with the FASTER device. The L7-4 transducer was mounted on the same linear and rotary positioners to scan the 3-D field, and thus, the 4-D (3-D space and time) scanning field can be accurately obtained. The sweeping motion of the transmitted beam was fit using a sinusoidal function to match the sinusoidal driving signal of the fast-tilting reflector. By fitting the dynamic sweeping beams at different depths, the scanning characteristics (i.e., amplitude, initial phase, and offset) of the fast-tilting reflector were calibrated, enabling accurate volumetric reconstruction using the FASTER 3-D imaging device.

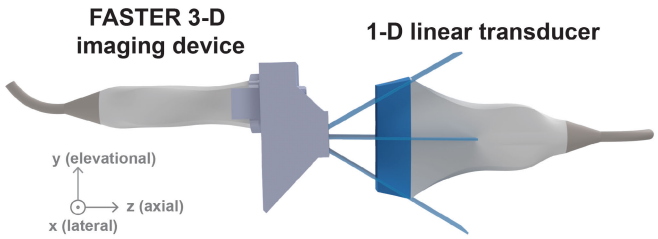

Fig. 3. Experimental setup of the acoustic calibration study for the FASTER 3-D imaging device. A second 1-D linear transducer (L7-4) was used to measure the dynamic 4-D scanning field of the FASTER device.

D. In Vitro Volumetric Imaging Studies

1) Three-Dimensional B-Mode Imaging: To quantitatively evaluate the imaging performance of the new FASTER device, a wire phantom (tungsten 99.95%, 100 μm diameter, four wires, and 3-mm spacing) and a home-made tissue-mimicking phantom with an anechoic cylindrical cyst were imaged by the FASTER device attached to the GE 9LD transducer. Spatial resolution and contrast-to-noise ratio (CNR) were used as quantitative metrics for evaluation. The frequency of the fast-tilting reflector was 150 Hz, resulting in a volume rate of 300 Hz as each scanning position was passed twice during one scanning cycle. For benchmarking, a mechanical translation-based 3-D image was captured to mimic that from a wobbler probe. The mechanical translation was precisely controlled by using a positing system (Daedal, Inc., Harrison City, PA, USA). A 0.5-mm step size was used along the elevational direction for the mechanical translation. The scanning volume rate was limited to approximately 0.1 Hz due to the scanning speed limitation of the Daedal system. The spatial resolution was characterized using the FWHM measured from the cross-sectional profiles of the wire targets. Fig. 4 shows the imaging setups, and the imaging parameters are summarized in Table II.

2) Three-Dimensional PD Imaging: An in vitro 3-D PD study was performed using a cross-shaped flow phantom (1.48 mm diameter) with flowing microbubbles (Definity, concentration of 1.2×10^6 MBs/mL, Lantheus Medical Imaging, Inc., North Billerica, MA, USA). The detailed procedures of

TABLE II
FASTER 3-D IMAGING PARAMETERS

Parameter	Value
Central frequency [MHz]	5.2
Bandwidth [%]	75
Number of elements	192
PRF [Hz]	9000
Volume Rate [Hz]	300
Fast-tilting reflector tilting frequency [Hz]	150
Scanning range [°]	±24.8
Distance from the fast-tilting reflector to the transducer [mm]	23.8
Imaging depth [mm]	60.0
Lateral (x) range [mm]	44.2
Elevational (y) range [mm]	33.5

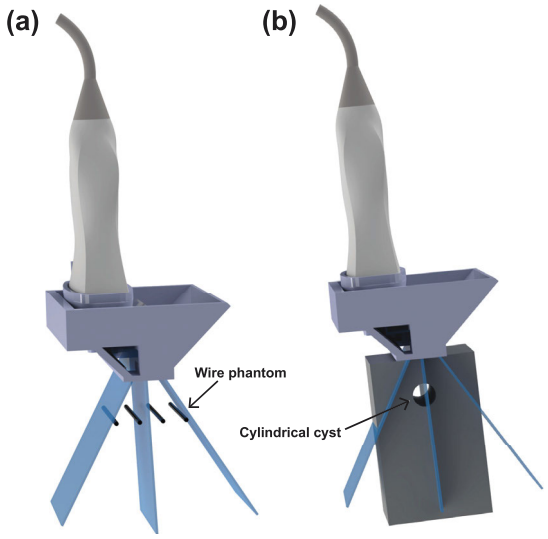

Fig. 4. (a) Experimental setup of the wire phantom imaging study and (b) tissue-mimicking phantom imaging study using the FASTER 3-D imaging device.

flow phantom making can be found in our previous work [32]. A constant flow velocity of 20 mm/s was used in this experiment. The imaging configurations were similar to the previous B-mode phantom study except that the frequency of the fast-tilting reflector was changed to 125 Hz with a PRF of 8000 Hz, which is equal to a 250-Hz volume rate. A total of 500 volumes were acquired with a 2-s acquisition time. Clutter filtering based on the singular value decomposition (SVD) [33] was performed on the reconstructed in-phase and quadrature (IQ) volumes, which were integrated to construct the 3-D PD image.

3) Three-Dimensional Super-Resolution ULM: To further demonstrate the high-volume-rate imaging capability of the FASTER device, an in vitro 3-D ULM study was performed using the same cross-shaped flow phantom and imaging configurations as the 3-D PD study. A total of 5500 volumes were acquired and beamformed, followed by SVD clutter filtering and 3-D microbubble localization using the radial symmetry

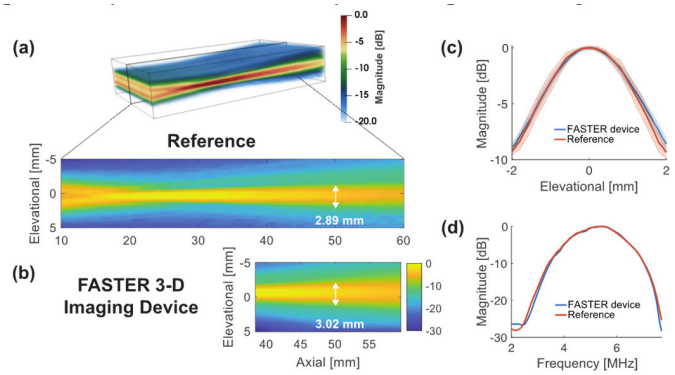

Fig. 5. Acoustic validation study results for the FASTER 3-D imaging device. (a) Representative beam profile plots in the elevational–axial plane for the direct acoustic field measurement from the transducer (without FASTER device) and (b) acoustic field of the FASTER device after the reflections by the redirecting reflector and fast-tilting reflector. The elevational beamwidths at 50-mm depth are labeled. (c) Plots of the beam profiles along the elevational dimension at 50-mm depth for reference and the FASTER device. (d) Comparisons of the spectrum of the acoustic fields with and without (reference) the FASTER device.

method [34], [35]. Finally, the trajectories of paired microbubbles across volumes were retrieved using 3-D particle tracking algorithms [36] and accumulated into the final 3-D ULM intensity map. The 3-D flow velocity map was also calculated based on the microbubble trajectories. A voxel size of 46 μm along three dimensions was used for the ULM intensity and velocity maps.

E. In Vivo Volumetric Imaging Study

An in vivo study was performed on the basilic vein of a healthy volunteer. The same clinical GE 9LD ultrasound transducer with the FASTER device was used for imaging, and the imaging configurations were the same as the in vitro 3-D B-mode study (Table II). To accommodate the speed of sound difference between acoustic medium and human tissue (e.g., 1480 versus 1540 m/s), the volumetric image was reconstructed using a customized delay-and-sum (DAS) beamforming, in which the delay was calculated using the fast marching method (FMM) by modeling a two-layer speed of sound map [37].

III. RESULTS

A. Acoustic Validation Study of Ultrasound Beam Reflections

Fig. 5 shows the acoustic beam characterizations between the reference acoustic field (without the FASTER device) and the acoustic field with the FASTER device. The acoustic field from the FASTER device was close to the reference acoustic field [see Fig. 5(a) and (b)] without significant distortion from beam reflections. The elevational beam profile, as well as the beamwidth of the FASTER device, remained similar to the reference. For example, the FWHM of the reference acoustic field was 2.89 mm at 50-mm axial depth, and that of the FASTER device was 3.02 mm, as shown in Fig. 5(c). Furthermore, the spectrum of the acoustic field was consistent between the reference and FASTER device, as shown in Fig. 5(d).

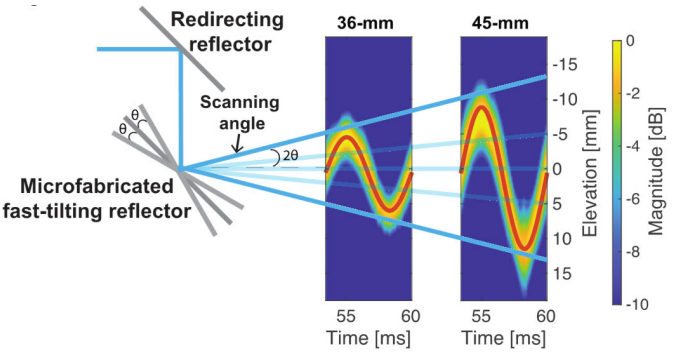

Fig. 6. Acoustic calibration study results for the FASTER 3-D imaging device. Acoustically measured elevational beam intensities were plotted over time at 36- and 45-mm depths. Low-pass filtering and windowing were applied to the raw radio frequency (RF) data acquired by the L7-4 transducer, and sinusoidal fitting was used on the beam intensity over time to characterize the dynamic scanning of the FASTER device.

The beam characterizations show that the reflectors did not significantly distort the acoustic signals in the context of beamwidth and frequency response. This result can be attributed to the high reflection coefficient of the silicon wafer and the precise alignment between the ultrasound probe and the reflectors [see Fig. 1(c)]. Such precise alignment was made possible by the careful assembly of the clip-on housing device.

B. Acoustic Calibration Study for Ultrasound Beam Scanning

Fig. 6 shows acoustic calibration results, including two transmitted beams measured at 36- and 45-mm axial depth over time. The sweeping motion of the transmitted beam was well matched with the sinusoidal driving signal of the fast-tilting reflector (red fit curve). As shown in Fig. 6, through using the fit sweeping motion measured at different axial locations, the scanning angle of the fast-tilting reflector was estimated as $\pm 24.8^\circ$ with an initial position of -0.2°.

C. In Vitro Volumetric Imaging Studies

1) Three-Dimensional B-Mode Imaging: Fig. 7 shows the wire phantom imaging results using the FASTER 3-D imaging device and the simulated wobbler 3-D scanning based on mechanical translation. The four wires imaged using the FASTER device were accurately reconstructed and clearly isolated from each other. The image from the FASTER device shows good agreement with that from the mechanical translation. The elevational FWHM of the wire imaged by the FASTER device was 1.73 ± 0.06 mm, and the one imaged by the linear scanning method was 1.9 ± 0.2 mm. The wire phantom imaging results demonstrated that the proposed FASTER device using both redirecting and fast-tilting reflectors provides comparable elevational resolution to the reference wobbler scanning method but with much higher volume rates (e.g., 300 Hz for FASTER versus ~0.1 Hz for mechanical translation).

Fig. 8 shows the tissue-mimicking phantom results using the FASTER 3-D imaging device and the simulated wobbler 3-D scanning. From both the 3-D volumetric rendering and

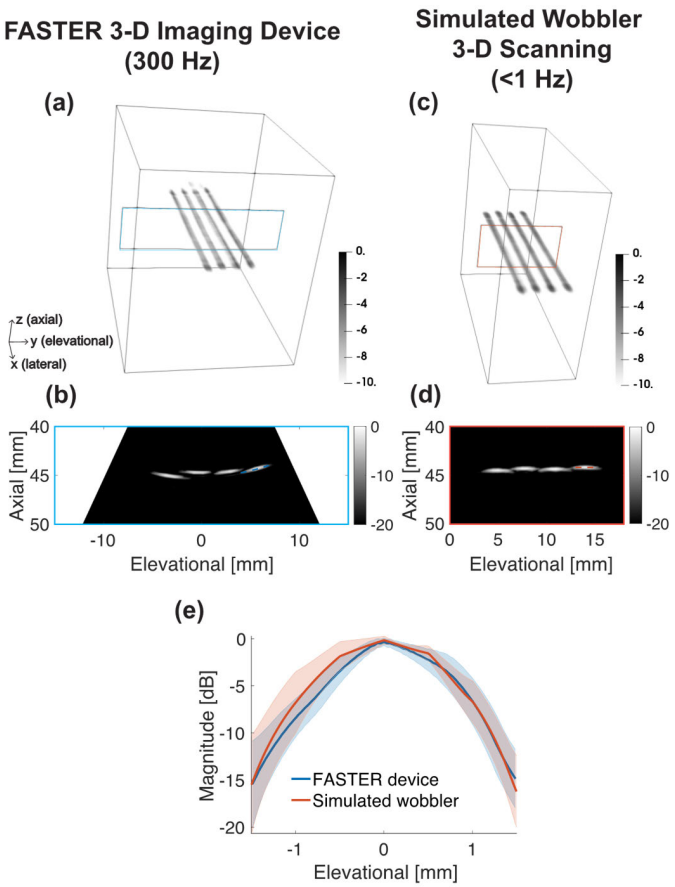

Fig. 7. Wire phantom imaging results using the FASTER 3-D imaging device and the simulated wobbler. (a) Reconstructed volumetric image of the wire phantom using the FASTER 3-D imaging device at a 300-Hz volume rate. (b) Elevational–axial image of the wire phantom using the FASTER 3-D imaging device. (c) Reconstructed volumetric image of the wire phantom using the simulated wobbler. (d) Elevational–axial image of the wire phantom using the simulated wobbler scanning. (e) Elevational profiles of the wire imaged by the FASTER 3-D imaging device and the simulated wobbler probe, corresponding ROIs are labeled in (b) and (d), and standard deviation (shaded area) was calculated across different lateral locations.

2-D images in Fig. 8, we can clearly see an anechoic cyst reconstructed with high contrast to the background using both methods. The CNR of the anechoic cyst imaged by the FASTER device was 1.52, and the reference CNR value by the scanning method was 1.56. The cyst-like inclusion phantom results showed that the FASTER device could provide similar imaging performance in the context of contrast to the benchmark method.

2) Three-Dimensional PD Imaging: Fig. 9(a) and (b) shows the reconstructed PD image of the cross-shaped flow phantom using the FASTER 3-D imaging device, where the two flow channels that are orthogonal to each other are clearly perceived. The measured lateral FWHM of the cross section of the flow channel located at 45-mm depth was 1.47 mm, as shown in Fig. 9(g). The 3-D PD imaging study illustrated the potential capability of contrast-free blood flow imaging with the FASTER device.

3) Three-Dimensional Super-Resolution ULM: Fig. 9(c)–(e) shows the reconstructed ULM intensity map and flow velocity

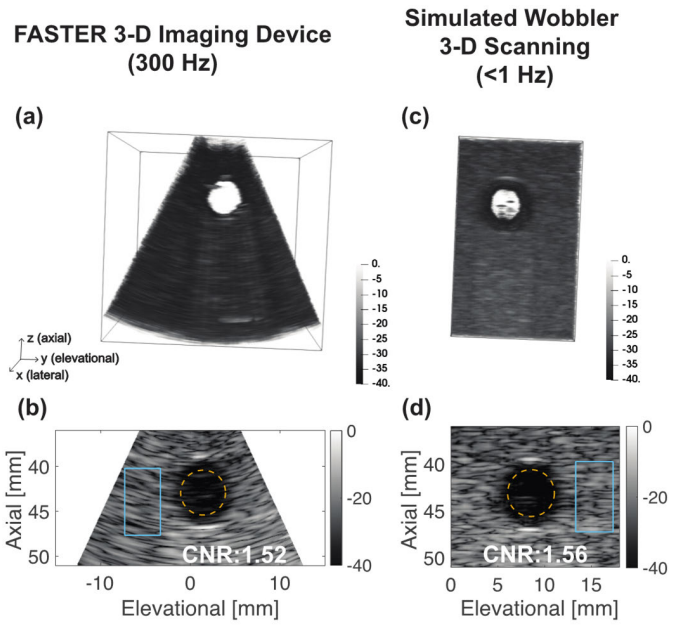

Fig. 8. Tissue-mimicking phantom imaging results using the FASTER 3-D imaging device and simulated wobbler 3-D scanning. (a) Reconstructed volumetric image of the tissue-mimicking phantom using the FASTER 3-D imaging device at a 300-Hz volume rate. (b) Elevational–axial image of the tissue-mimicking phantom using the FASTER 3-D imaging. (c) Reconstructed volumetric image of the tissue-mimicking phantom using simulated wobbler 3-D scanning. (d) Elevational–axial image of the tissue-mimicking phantom using simulated wobbler 3-D scanning. The ROIs for CNR calculation are labeled in (b) and (d) with calculated CNR values.

map of the cross-shaped flow phantom using the FASTER 3-D imaging device. The two perpendicular flow channels were clearly reconstructed with flow velocity estimation at a much higher spatial resolution. The mean velocity across all voxels was 26 ± 7 mm/s, which was higher than the nominal flow speed setup (20 mm/s), as shown in Fig. 9(f). One possible reason is that the gelatin-made flow channels may have been compressed slightly during acoustic coupling, resulting in a reduced luminal diameter and a higher flow speed inside the channels. The measured lateral FWHM of the same flow channel located at 45-mm depth was 0.65 mm [Fig. 9(g)], which was more than twofold improvement compared to the 3-D PD imaging results. However, it should be noted that FWHM may not be an appropriate metric for ULM to measure the flow channel diameter due to the stochastic nature of microbubble trajectory reconstruction. The 3-D ULM imaging study demonstrated the promising capability of applying advanced imaging techniques that need high-speed 3-D motion tracking with the FASTER device.

D. In Vivo Volumetric Imaging Study

Fig. 10 shows the in vivo imaging results using the FASTER 3-D imaging device on a healthy volunteer. The basilic vein was imaged, which can be clearly observed from the elevational–axial plane (cross-sectional view) and in the lateral–axial plane (longitudinal view) (arrows in Fig. 10). By providing volumetric data, any cross-sectional slicing of the vessel can be achieved, allowing for the quantification of physiological biomarkers such as vessel diameter and volume with anatomical context. A real-time biplanar B-mode imaging mode [Fig. 10(c)] provides a convenient and computationally efficient way of displaying 3-D volumetric data [38]. These results demonstrate the capability of in vivo human imaging using the FASTER device with a high volumetric imaging rate (e.g., 300 Hz).

IV. Discussion

Currently, 3-D ultrasound imaging is challenged by various technical limitations, such as low volume rate, high cost of equipment, and high computational complexities involved with beamforming and postprocessing. To address these issues, here, we proposed a novel 3-D imaging technique with high volumetric imaging rate—FASTER—which uses a fast-tilting reflector and a redirecting reflector to rapidly sweep plane waves in the elevational direction for high-speed 3-D scanning. Our results demonstrate that FASTER could achieve a high imaging volume rate (e.g., hundreds of hertz) and comparable imaging quality compared to conventional mechanical-translation-based 3-D scanning (e.g., wobbler). In addition, FASTER is based on conventional 1-D array transducers and can be conveniently adapted to existing ultrasound transducers, which takes advantage of the higher performance of linear arrays over matrix arrays. FASTER also enjoys a lightweight and compact form factor that is user-friendly. These advantages of FASTER pave the way for future clinical translations of the technology.

The previous FASTER solution changed the incident beam direction to 90° (i.e., from axial to elevational), which makes it challenging to perform handheld scanning. In this article, we improved the FASTER technique by incorporating a redirecting reflector to recover the original incident beam direction, which allows the transducer to be held in a regular position (e.g., upright). The validation study demonstrated that there were no significant beam distortions introduced by the new redirecting reflector. Regarding the beam reflection during the fast tilting, the fast-tilting reflector remains relatively stable due to the short pulselength (e.g., 0.2 μs) compared to the tilting cycle (e.g., 6666.7 μs), ensuring that the transmitted beam remains undistorted. For receiving, the fast-tilting reflector's tilted angle during the pulse echo (e.g., a maximum of 1.2° for a 10 000 PRF) might reduce the sensitivity of received signals from deeper regions, and this needs to be further characterized and explored.

Another limitation of the previous FASTER technique was that the imaging had to be performed inside a water tank because of the need of water as an acoustic wave conducting medium, which is not a practical solution for in vivo imaging. To address this issue, a clip-on housing device was designed to enclose the acoustic medium together with the redirecting reflector and the fast-tilting reflector. The clip-on device can be conveniently attached to or removed from conventional 1-D ultrasound probes. To avoid leakage of the acoustic medium, an acoustic film was sealed on the bottom of the device. The clip-on housing device frame can be easily fabricated using 3-D printing with biocompatible materials at a low cost, and the entire clip-on device is lightweight (57 g).

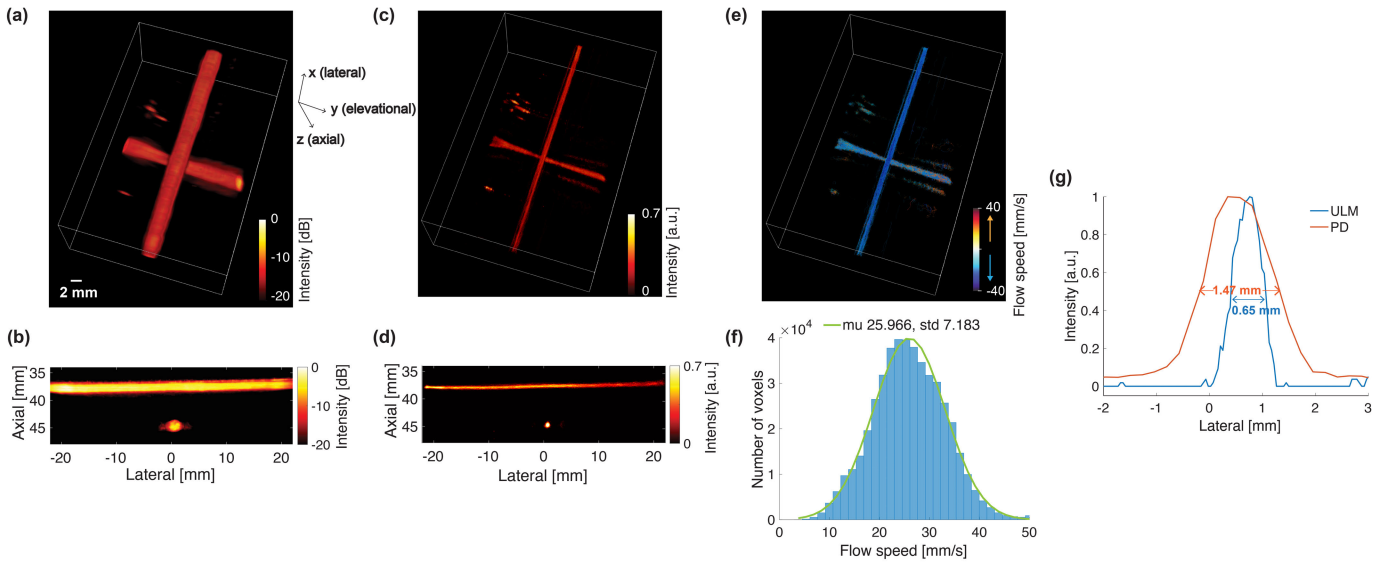

Fig. 9. Three-dimensional PD imaging and 3-D super-resolution ULM imaging of the cross-shaped flow phantom using the FASTER 3-D imaging device. (a) Reconstructed volumetric PD image of the flow phantom. (b) Lateral–axial PD image. (c) Reconstructed volumetric ULM intensity map of the flow phantom. The map was compressed with a cubic root for enhanced visibility. (d) Lateral–axial ULM intensity map (1-mm thickness and summation projection). (e) Reconstructed volumetric ULM flow velocity map of the flow phantom. (f) Flow velocity histogram of the flow phantom with a Gaussian fit curve (the mean is 25.97 mm/s and the standard deviation is 7.18 mm/s). (g) PD and ULM intensity profiles along the lateral dimension of the flow channel located at 45-mm depth.

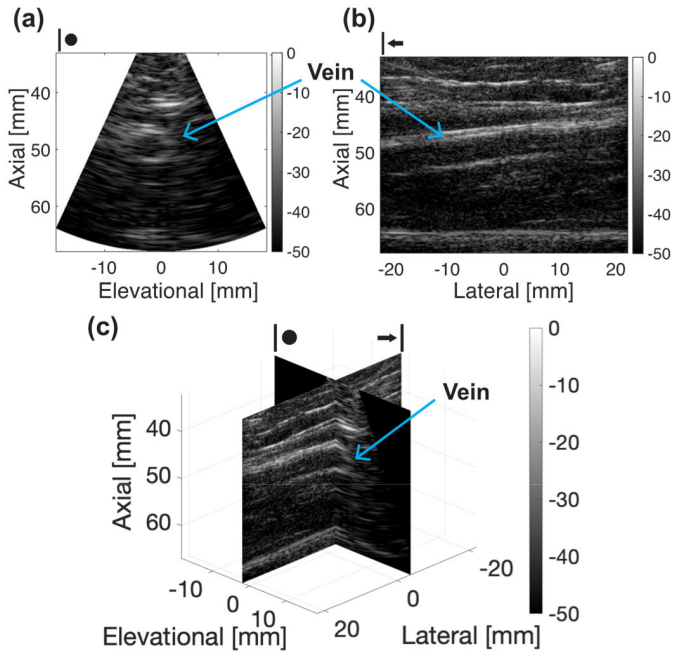

Fig. 10. In vivo 3-D imaging of the basilic vein from a healthy volunteer using the FASTER 3-D imaging device. (a) Out-of-plane (elevational–axial) image of the vein. (b) In-plane (lateral–axial) image of the vein. (c) Biplane view of the vein.

The in vitro phantom imaging studies showed that the newly developed FASTER 3-D imaging device provided comparable spatial resolution and contrast while maintaining a large FOV (e.g., 50° scanning angle) and a high volume rate (e.g., 300 Hz). The in vivo study showed the possibility of using the FASTER device for in vivo human imaging. Multiple imaging modalities, including B-mode, PD, and ULM, were demonstrated. The flow phantom study showcased the potential of applying advanced imaging techniques (3-D ULM and possibly 3-D SWE) using the new FASTER device. These results suggest that FASTER not only provides a viable solution for accessible 3-D ultrasound imaging but also has the potential to maintain and extend the functionality of 2-D ultrasound imaging to 3-D.

The current implementation of FASTER 3-D imaging requires synchronization between the tilting reflectors and the ultrasound system for accurate image reconstruction. For easier translation of the FASTER 3-D technology, an asynchronous acquisition mode is also feasible by using the correlation between consecutively acquired frames to estimate the scanning beam position. For example, the correlation coefficient between adjacent 2-D frames is the highest when the scanning angle is the largest (the scanning speed is the lowest) and vice versa. The asynchronous acquisition capability should greatly reduce the burden of potential system modifications to allow FASTER to be implemented on existing commercial ultrasound systems.

There are many other advanced ultrasound imaging techniques that can be benefited from high volumetric imaging rates enabled by the FASTER device. For example, 3-D SWE is essential for accurate and comprehensive tissue stiffness measurement. However, 3-D SWE (acoustic radiation force-based) is difficult to achieve because of the need for a high 3-D imaging volume rate and transmitting the high-power push beams. Wobblers do not provide an adequate 3-D volume rate for shear wave tracking, while 2-D matrix arrays do not typically support the transmission of long-duration, high mechanical index (MI) push pulses for shear wave generation. In comparison, FASTER provides a potentially viable solution for 3-D SWE because it supports high-volume-rate

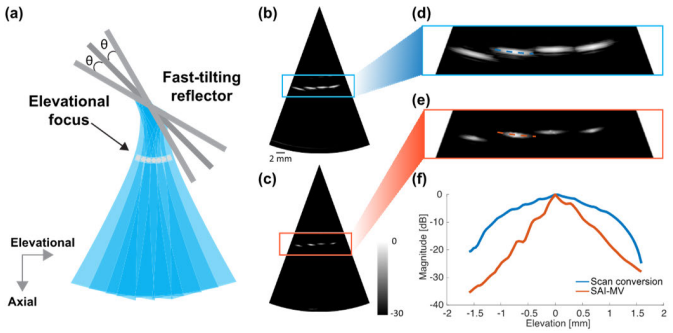

Fig. 11. Proof-of-concept study of applying SAI on FASTER 3-D imaging to improve elevational resolution using a double-reflector setup in the water tank, and the beam was reflected by a fast-tilting reflector first and then by redirecting reflector. (a) Schematic for taking advantage of elevational focus as virtual sources in FASTER 3-D imaging to enable synthetic aperture-based beamforming, the redirecting reflector was not shown for better visualization. (b) Elevational–axial image of the wire phantom reconstructed using conventional scan conversion method. (c) Elevational–axial image reconstructed using elevational SAI combined with MV beamforming (SAI-MV). (d) Magnified region of the wire phantom image using conventional scan conversion. (e) Magnified region of the wire phantom image using SAI-MV. (f) Elevational profile comparison of the wire phantom between scan conversion and SAI-MV, as indicated in (d) and (e).

3-D scanning and it uses conventional 1-D ultrasound transducers that are compatible with ARF-based SWE. Although the volume rate of the current FASTER device (e.g., 300 Hz) is not adequate for 3-D SWE, ongoing studies are being conducted to increase the tilting frequency of the reflector for 3-D shear wave tracking (e.g., to 2 kHz).

Similar to other 1-D array-based 3-D imaging methods, out-of-plane signals were not utilized in FASTER 3-D imaging, and the elevational resolution is determined by the elevational beamwidth. To enhance the FASTER 3-D imaging quality, a virtual array along the elevational dimension can be constructed using the elevational focuses of different scanning beams, as shown in Fig. 11(a). Consequently, synthetic aperture imaging (SAI) can be employed to achieve the elevational focus and improve the elevational resolution [39], [40]. Furthermore, adaptive beamforming methods, such as minimum variance (MV) [41] or general coherent factor (GCF) [42], can be applied to further enhance the elevational resolution. A proof-of-concept study was conducted on a wire phantom in the water tank using a double-reflector setup in which acoustic beams were reflected by the fast-tilting reflector first and then by the redirecting reflector. The elevational focus of the elevational beam was ensured to be beyond the fast-tilting reflector and distributed at different elevational locations to form the virtual array. Fig. 11(b)–(f) shows the reconstruction comparison between the conventional scan conversion and SAI combined with MV, from which we can see that the wire phantom was successfully constructed, and the elevational resolution was significantly improved (e.g., 1.78 to 0.58 mm at −6 dB). The SAI method will be fully implemented on the FASTER device in future studies.

In addition to PD and ULM studies demonstrated in the article, other advanced modes, such as color Doppler, could also be applied using a FASTER device. However, for accurate blood flow velocity measurement, the effects of elevational beamwidth need to be considered, and appropriate characterization and compensation are necessary. Furthermore, for clinical color Doppler applications, the reflector tilting frequency also needs to be increased.

One limitation in current ULM imaging with the FASTER device was that a spatially invariant PSF was used for microbubble localization. However, the PSF of the FASTER 3-D imaging system is spatially varying, for example, the elevational resolution was reduced in deeper imaging depth [Fig. 5(b)], and the elevational PSF was tilted correspondingly to the scanning angle, as shown in Fig. 7(b). As a result, a spatially varying PSF needs to be characterized and employed for optimized microbubble location in future work, for example, deep learning methods can be applied to characterize microbubble PSF and address this problem [43].

The acoustic film in the current device design was made with PVC with a thickness of 0.01 mm. The acoustic impedance mismatch between the PVC acoustic film and the acoustic conducting medium (e.g., water) may result in reverberation artifacts for FASTER. Future work will be conducted to fabricate acoustic films using biocompatible materials with reduced reverberation and membrane thickness.

In addition to the impedance mismatch between the acoustic film and the acoustic medium, there was a slight speed of sound mismatch between the acoustic medium and soft tissue for in vivo imaging. To address this issue, a two-layer speed of sound map was used in the DAS beamforming process based on the FMM [37] for the in vivo imaging study. An alternative solution is to switch to an acoustic wave conduction medium with a similar speed of sound of soft tissue.

V. Conclusion

In this work, we introduced an improved FASTER 3-D imaging method by incorporating a redirecting reflector to facilitate the convenient handling of the ultrasound probe. We also developed a compact and lightweight clip-on housing device that can be easily adapted to conventional 1-D transducers. The phantom imaging studies demonstrated that the FASTER 3-D imaging device provided comparable imaging quality to the conventional, mechanical-translation-based 3-D imaging (i.e., wobbler) while providing a much higher 3-D imaging volume rate. The utility of the new FASTER device was also tested in an in vivo case study for 3-D B-mode imaging. The proposed methods in this study could clear key hurdles for the application of FASTER in regular ultrasound imaging settings for high-speed and high-quality 3-D ultrasound imaging.

Acknowledgment

The content is solely the responsibility of the authors and does not necessarily represent the official views of the National Institutes of Health.

Zhijie Dong and Matthew R. Lowerison are with the Department of Electrical and Computer Engineering, Beckman Institute for Advanced Science and Technology, University of Illinois Urbana-Champaign, Urbana, IL 61801 USA (e-mail: zhijied3@illinois.edu; mloweri@illinois.edu).

Shuangliang Li, Xiaoyu Duan, and Jun Zou are with the Department of Electrical and Computer Engineering, Texas A&M University, College Station, TX 77843 USA (e-mail: slli940922@tamu.edu; duanxiaoyu@tamu.edu; junzou@tamu.edu).

Chengwu Huang and Shigao Chen are with the Department of Radiology, Mayo Clinic College of Medicine and Science, Rochester, MN 55905 USA (e-mail: huang.chengwu@mayo.edu; chen.shigao@mayo.edu).

Qi You is with the Department of Bioengineering, Beckman Institute for Advanced Science and Technology, University of Illinois Urbana–Champaign, Urbana, IL 61801 USA (e-mail: qiyou3@illinois.edu).

Pengfei Song is with the Department of Electrical and Computer Engineering and the Department of Bioengineering, Beckman Institute for Advanced Science and Technology, Carle Illinois College of Medicine, Cancer Center at Illinois, and the Neuroscience Program at the University of Illinois Urbana-Champaign, Urbana, IL 61801 USA (e-mail: songp@illinois.edu).

REFERENCES

[1] B. Delannoy, R. Torguet, C. Bruneel, E. Bridoux, J. M. Rouvaen, and H. Lasota, "Acoustical image reconstruction in parallel-processing analog electronic systems," *J. Appl. Phys.*, vol. 50, no. 5, pp. 3153–3159, May 1979.

[2] D. P. Shattuck, M. D. Weinshenker, S. W. Smith, and O. T. von Ramm, "Explososcan: A parallel processing technique for high speed ultrasound imaging with linear phased arrays," *J. Acoust. Soc. Amer.*, vol. 75, no. 4, pp. 1273–1282, Apr. 1984.

[3] G. Montaldo, M. Tanter, J. Bercoff, N. Benech, and M. Fink, "Coherent plane-wave compounding for very high frame rate ultrasonography and transient elastography," *IEEE Trans. Ultrason., Ferroelectr., Freq. Control*, vol. 56, no. 3, pp. 489–506, Mar. 2009.

[4] M. Tanter and M. Fink, "Ultrafast imaging in biomedical ultrasound," *IEEE Trans. Ultrason., Ferroelectr., Freq. Control*, vol. 61, no. 1, pp. 102–119, Jan. 2014.

[5] J. Bercoff, M. Tanter, and M. Fink, "Supersonic shear imaging: A new technique for soft tissue elasticity mapping," *IEEE Trans. Ultrason., Ferroelectr., Freq. Control*, vol. 51, no. 4, pp. 396–409, Apr. 2004.

[6] P. Song et al., "Two-dimensional shear-wave elastography on conventional ultrasound scanners with time-aligned sequential tracking (TAST) and comb-push ultrasound shear elastography (CUSE)," *IEEE Trans. Ultrason., Ferroelectr., Freq. Control*, vol. 62, no. 2, pp. 290–302, Feb. 2015.

[7] E. Macé, G. Montaldo, I. Cohen, M. Baulac, M. Fink, and M. Tanter, "Functional ultrasound imaging of the brain," *Nature Methods*, vol. 8, pp. 662–664, May 2011.

[8] C. Errico et al., "Ultrafast ultrasound localization microscopy for deep super-resolution vascular imaging," *Nature*, vol. 527, no. 7579, pp. 499–502, Nov. 2015.

[9] N. Renaudin, C. Demené, A. Dizeux, N. Ialy-Radio, S. Pezet, and M. Tanter, "Functional ultrasound localization microscopy reveals brain-wide neurovascular activity on a microscopic scale," *Nature Methods*, vol. 19, no. 8, pp. 1004–1012, Aug. 2022.

[10] R. W. Gill, "Measurement of blood flow by ultrasound: Accuracy and sources of error," *Ultrasound Med. Biol.*, vol. 11, no. 4, pp. 625–641, Jul. 1985.

[11] J. Gennisson et al., "4-D ultrafast shear-wave imaging," *IEEE Trans. Ultrason., Ferroelectr., Freq. Control*, vol. 62, no. 6, pp. 1059–1065, Jun. 2015.

[12] G. Unsgaard, S. Ommedal, T. M´uller, A. Gronningsaeter, and T. A. N. Hernes, "Neuronavigation by intraoperative three-dimensional ultrasound: Initial experience during brain tumor resection," *Neurosurgery*, vol. 50, no. 4, pp. 804–812, Apr. 2002.

[13] D. C. D. A. Bastos et al., "Challenges and opportunities of intraoperative 3D ultrasound with neuronavigation in relation to intraoperative MRI," *Frontiers Oncol.*, vol. 11, May 2021, Art. no. 656519.

[14] T. Lange et al., "3D ultrasound-CT registration of the liver using combined landmark-intensity information," *Int. J. Comput. Assist. Radiol. Surg.*, vol. 4, no. 1, pp. 79–88, Jan. 2009.

[15] H. Neshat, D. W. Cool, K. Barker, L. Gardi, N. Kakani, and A. Fenster, "A 3D ultrasound scanning system for image guided liver interventions," *Med. Phys.*, vol. 40, no. 11, Oct. 2013, Art. no. 112903.

[16] M. V. Burri, D. Gupta, R. E. Kerber, and R. M. Weiss, "Review of novel clinical applications of advanced, real-time, 3-dimensional echocardiography," *Transl. Res.*, vol. 159, no. 3, pp. 149–164, Mar. 2012.

[17] P. Acar et al., "Real-time three-dimensional foetal echocardiography using a new transabdominal xMATRIX array transducer," *Arch. Cardiovascular Diseases*, vol. 107, no. 1, pp. 4–9, Jan. 2014.

[18] R. Chaoui, A. Abuhamad, J. Martins, and K. S. Heling, "Recent development in three and four dimension fetal echocardiography," *Fetal Diagnosis Therapy*, vol. 47, no. 5, pp. 345–353, 2020.

[19] A. Fenster, K. Surry, W. Smith, and D. B. Downey, "The use of three-dimensional ultrasound imaging in breast biopsy and prostate therapy," *Measurement*, vol. 36, nos. 3–4, pp. 245–256, Oct. 2004.

[20] M. Correia, J. Provost, M. Tanter, and M. Pernot, "4D ultrafast ultrasound flow imaging: In vivo quantification of arterial volumetric flow rate in a single heartbeat," *Phys. Med. Biol.*, vol. 61, no. 23, pp. L48–L61, Dec. 2016.

[21] R. W. Prager, U. Z. Ijaz, A. Gee, and G. M. Treece, "Three-dimensional ultrasound imaging," *Proc. Inst. Mech. Eng., H, J. Eng. Med.*, vol. 224, no. 2, pp. 193–223, 2010.

[22] J. T. Yen and S. W. Smith, "Real-time rectilinear 3-D ultrasound using receive mode multiplexing," *IEEE Trans. Ultrason., Ferroelectr., Freq. Control*, vol. 51, no. 2, pp. 216–226, Feb. 2004.

[23] S. Blaak et al., "Design of a micro-beamformer for a 2D piezoelectric ultrasound transducer," in *Proc. IEEE Int. Ultrason. Symp.*, Sep. 2009, pp. 1338–1341.

[24] E. Roux, F. Varray, L. Petrusca, C. Cachard, P. Tortoli, and H. Liebgott, "Experimental 3-D ultrasound imaging with 2-D sparse arrays using focused and diverging waves," *Sci. Rep.*, vol. 8, no. 1, pp. 1–12, Jun. 2018.

[25] C. E. Morton and G. R. Lockwood, "Theoretical assessment of a crossed electrode 2-D array for 3-D imaging," in *Proc. IEEE Symp. Ultrason.*, Oct. 2003, pp. 968–971.

[26] J. A. Jensen et al., "Three-dimensional super-resolution imaging using a row–column array," *IEEE Trans. Ultrason., Ferroelectr., Freq. Control*, vol. 67, no. 3, pp. 538–546, Mar. 2020.

[27] J. Sauvage et al., "4D functional imaging of the rat brain using a large aperture row-column array," *IEEE Trans. Med. Imag.*, vol. 39, no. 6, pp. 1884–1893, Jun. 2020.

[28] Z. Dong et al., "Three-dimensional shear wave elastography using a 2D row column addressing (RCA) array," *BME Frontiers*, vol. 2022, Jan. 2022, Art. no. 9879632.

[29] Z. Dong, S. Li, M. R. Lowerison, J. Pan, J. Zou, and P. Song, "Fast acoustic steering via tilting electromechanical reflectors (FASTER): A novel method for high volume rate 3-D ultrasound imaging," *IEEE Trans. Ultrason., Ferroelectr., Freq. Control*, vol. 68, no. 3, pp. 675–687, Mar. 2021.

[30] C.-H. Huang, J. Yao, L. V. Wang, and J. Zou, "A water-immersible 2-axis scanning mirror microsystem for ultrasound andha photoacoustic microscopic imaging applications," *Microsyst. Technol.*, vol. 19, no. 4, pp. 577–582, Apr. 2013.

[31] I. Amidror, "Scattered data interpolation methods for electronic imaging systems: A survey," *J. Electron. Imag.*, vol. 11, no. 2, pp. 157–176, 2002.

[32] X. Chen et al., "Localization free super-resolution microbubble velocimetry using a long short-term memory neural network," *IEEE Trans. Med. Imag.*, early access, Mar. 1, 2023, doi: 10.1109/TMI.2023.3251197.

[33] J. Baranger, B. Arnal, F. Perren, O. Baud, M. Tanter, and C. Demené, "Adaptive spatiotemporal SVD clutter filtering for ultrafast Doppler imaging using similarity of spatial singular vectors," *IEEE Trans. Med. Imag.*, vol. 37, no. 7, pp. 1574–1586, Jul. 2018.

[34] B. Heiles et al., "Volumetric ultrasound localization microscopy of the whole rat brain microvasculature," *IEEE Open J. Ultrason., Ferroelectr., Freq. Control*, vol. 2, pp. 261–282, 2022.

[35] R. Parthasarathy, "Rapid, accurate particle tracking by calculation of radial symmetry centers," *Nature Methods*, vol. 9, no. 7, pp. 724–726, Jul. 2012.

[36] K. Jaqaman et al., "Robust single-particle tracking in live-cell time-lapse sequences," *Nature Methods*, vol. 5, no. 8, pp. 695–702, Aug. 2008.

[37] J. A. Sethian, "Fast marching methods," *SIAM Rev.*, vol. 41, no. 2, pp. 199–235, Jan. 1999.

[38] D. Convissar, E. A. Bittner, and M. G. Chang, "Biplane imaging versus standard transverse single-plane imaging for ultrasound-guided peripheral intravenous access: A prospective controlled crossover trial," *Crit. Care Explor.*, vol. 3, no. 10, p. e545, 2021.

[39] S. I. Nikolov, *Synthetic Aperture Tissue and Flow Ultrasound Imaging. Center for Fast Ultrasound Imaging*. Lyngby, Denmark: Technical Univ. Denmark, 2002.

[40] Y. Tang, R. Tsumura, J. T. Kaminski, and H. K. Zhang, "Actuated reflector-based 3-D ultrasound imaging with synthetic aperture focusing," *IEEE Trans. Ultrason., Ferroelectr., Freq. Control*, vol. 69, no. 8, pp. 2437–2446, Aug. 2022.

[41] J.-F. Synnevag, A. Austeng, and S. Holm, "Benefits of minimum-variance beamforming in medical ultrasound imaging," *IEEE Trans. Ultrason., Ferroelectr., Freq. Control*, vol. 56, no. 9, pp. 1868–1879, Sep. 2009.

[42] P.-C. Li and M.-L. Li, "Adaptive imaging using the generalized coherence factor," *IEEE Trans. Ultrason., Ferroelectr., Freq. Control*, vol. 50, no. 2, pp. 128–141, Feb. 2003.

[43] Y. Shin et al., "Context-aware deep learning enables high-efficacy localization of high concentration microbubbles for super-resolution ultrasound localization microscopy," *BioRxiv*, Apr. 2023, doi: 10.1101/2023.04.21.536599.

Zhijie Dong (Graduate Student Member, IEEE) received the B.Eng. degree in information engineering from Southeast University, Nanjing, China, in 2017, and the M.S. degree in electrical and computer engineering from the University of Michigan, Ann Arbor, MI, USA, in 2018. He is currently pursuing the Ph.D. degree with the Department of Electrical and Computer Engineering, University of Illinois at Urbana–Champaign, Urbana, IL, USA.

His current research interests include ultrafast 3-D ultrasound imaging and deep learning in ultrasound.

Shuangliang Li received the B.S. degree in microelectronics science and engineering from East China Normal University, Shanghai, China, in 2017. He is currently pursuing the Ph.D. degree with the Department of Electrical Engineering, Texas A&M University, College Station, TX, USA.

His current research interests include MEMS scanning mirrors design and fabrication.

Xiaoyu Duan received the Ph.D. degree in electrical engineering from Texas A&M University, College Station, TX, USA, in 2022.

Her major research interests involve underwater optical and acoustic dual modal communication and ranging devices.

Matthew R. Lowerison received the Ph.D. degree in medical biophysics from the University of Western Ontario, London, ON, Canada, in 2017.

He is currently working with the Department of Electrical and Computer Engineering, Beckman Institute for Advanced Science and Technology, University of Illinois at Urbana–Champaign, Urbana, IL, USA. His current research interests include ultrasound microvessel imaging, super-resolution ultrasound localization microscopy, and ultrasonic characterization of tumor microenvironments.

Chengwu Huang received the B.S. degree in biomedical engineering from Beihang University, Beijing, China, in 2012, and the Ph.D. degree from the Department of Biomedical Engineering, Tsinghua University, Beijing, in 2017.

He is currently an Assistant Professor with the Department of Radiology, Mayo Clinic College of Medicine, Rochester, MN, USA. His current research interests include super-resolution ultrasound microvessel imaging, functional ultrasound imaging, Doppler ultrasound, and ultrasound elastography.

Qi You (Graduate Student Member, IEEE) received the B.S. and M.S. degrees in electronic science and engineering from Nanjing University, Nanjing, Jiangsu, China, in 2016 and 2019, respectively. He is currently pursuing the Ph.D. degree with the Department of Bioengineering, University of Illinois at Urbana–Champaign, Urbana, IL, USA.

His current research interests include ultrasound beamforming and super-resolution techniques.

Shigao Chen (Senior Member, IEEE) received the Ph.D. degree in biomedical imaging from the Mayo Graduate School, Rochester, MN, USA, in 2002.

He is currently a Professor of radiology with the Mayo Clinic College of Medicine, Rochester. His current research interests include ultrasound beamforming, shear wave elastography, liver steatosis quantification, and microvessel imaging.

Jun Zou (Senior Member, IEEE) received the Ph.D. degree in electrical engineering from the University of Illinois at Urbana–Champaign, Urbana, IL, USA, in 2002.

In 2004, he joined the Department of Electrical and Computer Engineering, Texas A&M University, College Station, TX, USA. He is currently a Full Professor and directs the Micro Imaging and Sensing Devices and Systems (MISDS) Laboratory with Texas A&M University. His current research interests include the development of micro and nano opto-electromechanical devices and systems for biomedical imaging, robotics, and artificial intelligence applications.

Dr. Zou is a Senior Member of the SPIE and a member of OSA.

Pengfei Song (Senior Member, IEEE) received the Ph.D. degree in biomedical engineering from the Mayo Clinic College of Medicine, Rochester, MN, USA, in 2014, under the supervision of Dr. James Greenleaf and Dr. Shigao Chen.

He is currently an Assistant Professor with the Department of Electrical and Computer Engineering and the Beckman Institute for Advanced Science and Technology, University of Illinois Urbana–Champaign, Urbana, IL, USA. He has authored and coauthored over 80 peer-reviewed journal articles in the field of ultrasound imaging. He holds several patents that have been licensed and commercialized by major ultrasound companies and used worldwide in the clinic. His current research interests include super-resolution ultrasound imaging, ultrafast 3-D imaging, deep learning, functional ultrasound, and ultrasound shear wave elastography.

Dr. Song was a recipient of the NIH K99/R00 Pathway to Independence Award, the NSF CAREER Award, and the NIH/NIBIB Trailblazer Award. He is a fellow of the American Institute of Ultrasound in Medicine, a Senior Member of the National Academy of Inventors, and a full member of ASA.